Nbn–Mre11 interaction is required for tumor suppression and genomic integrity

Jun Hyun Kim[a], Alexander V. Penson[b,c], Barry S. Taylor[b,c,d], and John H. J. Petrini[a,1]

[a]Molecular Biology Program, Memorial Sloan-Kettering Cancer Center, New York, NY 10065; [b]Human Oncology and Pathogenesis Program, Memorial Sloan-Kettering Cancer Center, New York, NY 10065; [c]Department Epidemiology and Biostatistics, Memorial Sloan-Kettering Cancer Center, New York, NY 10065; and [d]Center for Molecular Oncology, Memorial Sloan-Kettering Cancer Center, New York, NY 10065

Edited by Richard D. Kolodner, Ludwig Cancer Research, La Jolla, CA, and approved June 21, 2019 (received for review March 29, 2019)

We derived a mouse model in which a mutant form of Nbn/Nbs1^{mid8} (hereafter Nbn^{mid8}) exhibits severely impaired binding to the Mre11–Rad50 core of the Mre11 complex. The *Nbn^{mid8}* allele was expressed exclusively in hematopoietic lineages (in *Nbn$^{-/mid8vav}$* mice). Unlike *Nbn$^{flox/floxvav}$* mice with Nbn deficiency in the bone marrow, *Nbn$^{-/mid8vav}$* mice were viable. *Nbn$^{-/mid8vav}$* mice hematopoiesis was profoundly defective, exhibiting reduced cellularity of thymus and bone marrow, and stage-specific blockage of B cell development. Within 6 mo, *Nbn$^{-/mid8}$* mice developed highly penetrant T cell leukemias. *Nbn$^{-/mid8vav}$* leukemias recapitulated mutational features of human T cell acute lymphoblastic leukemia (T-ALL), containing mutations in *NOTCH1*, *TP53*, *BCL6*, *BCOR*, and *IKZF1*, suggesting that *Nbn^{mid8}* mice may provide a venue to examine the relationship between the Mre11 complex and oncogene activation in the hematopoietic compartment. Genomic analysis of *Nbn$^{-/mid8vav}$* malignancies showed focal amplification of 9qA2, causing overexpression of *MRE11* and *CHK1*. We propose that overexpression of *MRE11* compensates for the metastable Mre11–Nbn^{mid8} interaction, and that selective pressure for overexpression reflects the essential role of Nbn in promoting assembly and activity of the Mre11 complex.

Nbn–Mre11 interaction | genomic instability | DNA damage response | tumor suppression

The Mre11 complex, composed of Mre11, Rad50, and Nbn/Nbs1 (hereafter Nbn), is a sensor of DNA double-strand breaks (DSBs) and is required for the activation of the ATM axis of the DNA damage response (DDR) which parallels the ATR–Chk1 axis. The complex plays an integral role in all aspects of DSB repair (1), and its hypomorphic mutations are involved in rare human DNA repair disorders (2–4).

Several lines of evidence indicate that the Mre11 complex is critical for the process of DNA replication. Among them are the following: Mre11 complex components are physically associated with the replication fork in normal as well as stressed conditions (5), the complex is required for viability of proliferating cells but dispensable for that of quiescent cells (6), and the association of the complex with chromatin is qualitatively and quantitatively distinct in S phase compared with DNA damage-induced association (7, 8). These observations underscore the fact that, with respect to preserving genomic integrity, Mre11 complex plays a central role in the DNA replication in normal as well as pathologic states.

Whereas Mre11 and Rad50 orthologs are readily identifiable in all branches of life, Nbn (or Xrs2 in *Saccharomyces cerevisiae*) orthologs are found only in Eukarya (9). Nbn interacts with Mre11 via a bipartite domain near its C terminus (10). We previously derived a series of *Nbn* alleles that targeted the Nbn–Mre11 interface (called *Nbn^{mid}* mutants for Mre11 interaction domain) so that the functionality of Nbn in isolation from the core Mre11–Rad50 complex could be assessed. The *Nbn^{mid8}* allele, in which coding sequence for 4 amino acids is deleted from the Mre11 interaction domain (LKNFKKFKK; underlined amino acids deleted) was found to be embryonic lethal, and was unable to support the viability of immortalized murine embryonic fibroblasts (MEFs) (11). Conversely, a 108-amino acid fragment of Nbn that contained the bipartite Mre11 binding interface was sufficient to confer viability in MEFs as well as in the hematopoietic system (11). These data indicate that the essential function of Nbn is to stabilize and promote assembly of the active form of the Mre11–Rad50 core complex.

Nijmegen breakage syndrome (NBS) is a rare autosomal recessive disorder associated with microcephaly, immune deficiency, chromosomal instability, and cancer predisposition (12). About 95% of NBS patients are homozygous for a 657del5 truncating mutation in the *Nbn* gene, resulting in unstable expression of an N-terminal (Nbn^{p26}) and C-terminal fragment (Nbn^{p70}) (2, 13). The mouse model of human NBS (*Nbn$^{\Delta B}$*) showed identical phenotypes to that of NBS patients (14). The *Nbn$^{\Delta B}$* allele produces unstable Nbn^{p80} fragment lacking the forkhead-associated (FHA) and BRCA1 C-terminal (BRCT) domains, but containing an Mre11 interaction domain. These mutant cells are viable but exhibit defects in DSB end resection, DNA repair, and checkpoint, which are due to loss of FHA/BRCT interacting proteins (15–18). In contrast, mouse *Nbn1^{mid8}* allele produces the full-length protein save for 4 amino acids, which are deleted in the Mre11 interaction domain, but confers a substantially more severe phenotype than the *Nbn$^{\Delta B}$* or NBS patient cells.

In this study, we used a hematopoietic cell-specific *cre* (*cre^{vav}*) to test the hypothesis that the *Nbn^{mid8}* gene product specified sufficient residual function to support viability in the bone marrow (BM). The hematopoietic compartment was chosen for this experiment because it is dispensable for embryogenesis, and

Significance

The Mre11 complex core, consisting of Mre11, Rad50, and Nbn/Nbs1, is essential for viability. Accordingly, hematopoietic-specific Nbn deficiency leads to perinatal lethality. In contrast, destabilizing the interaction of Nbn with the core Mre11–Rad50 (*Nbn^{mid8}* allele) in hematopoietic cells permits viability but leads to severe defects in hematopoiesis. Viability requires gene amplification of *MRE11* and *CHK1*. We propose that the *MRE11* overexpression compensates for weakened Nbn interaction, and that selection for *CHK1* overexpression mitigates the genomic instability and loss of ATM-dependent checkpoint functions. The surviving animals develop highly penetrant T-ALL, the mutational features of which resemble human T-ALL. Hence, Nbn meets the definition of a tumor suppressor in this context.

Author contributions: J.H.K. and J.H.J.P. designed research; J.H.K. performed research; J.H.K. contributed new reagents/analytic tools; J.H.K., A.V.P., B.S.T., and J.H.J.P. analyzed data; and J.H.K., B.S.T., and J.H.J.P. wrote the paper.

The authors declare no conflict of interest.

This article is a PNAS Direct Submission.

[1]To whom correspondence may be addressed. Email: petrinij@mskcc.org.

This article contains supporting information online at www.pnas.org/lookup/suppl/doi:10.1073/pnas.1905305116/-/DCSupplemental.

Published online July 8, 2019.

even severe deficits in hematopoietic development are compatible with postnatal viability in mice. Also, we reasoned that, amid the abundant cellularity of the hematopoietic system, productive assemblies of Nbn^{mid8} with the Mre11–Rad50 core might occur at a sufficient frequency to promote the development of at least a pauciclonal hematopoietic compartment if Nbn^{mid8} retained some functionality.

In contrast to $Nbn^{flox/flox}$ mice, which, upon cre^{vav} expression, were Nbn-deficient in the BM and inviable, mice expressing Nbn^{mid8} in hematopoietic lineages were viable postnatally, albeit with severe defects in hematopoiesis, and decrements in the levels of all hematopoietic components. Nbn^{mid8} mice developed aggressive T cell malignancy which uniformly exhibited amplification and overexpression of *MRE11* as well as *CHK1* during the course of development and tumorigenesis. In $Nbn^{-/mid8}$ MEFs, cooverexpression of *MRE11* and *CHK1* was required for viability; overexpression of *MRE11* alone did not rescue $Nbn^{-/mid8}$ cellular lethality. The increased abundance of Mre11 appears to be required to mitigate the weakened interaction with Nbn^{mid8} in vivo. These data suggest that Nbn is essential for the assembly of a functional Mre11 complex.

Results

$Nbn^{-/mid8}$ vav^{cre} and Hematopoiesis. The Mre11 complex is required for hematopoiesis (6, 19–21). We asked whether the Nbn^{mid8} gene product had sufficient residual function to allow hematopoietic stem cells expressing only Nbn^{mid8} to support hematopoietic development.

Nbn^{mid8} mice were crossed with Nbn^{flox} mice (22) and vav^{cre} mice in which *cre* expression is restricted to hematopoietic stem cells (23) to create $Nbn^{-/mid8}$ vav^{cre} mice (hereafter $Nbn^{-/mid8vav}$ mice). For the experiments described below, control mice include $Nbn^{flox/+}$ vav^{cre} (hereafter $Nbn^{-/+vav}$) and $Atm^{floxflox}$ vav^{cre} (hereafter $Atm^{-/-vav}$). As expected, $Nbn^{-/-vav}$ mice, in which hematopoietic cells are completely Nbn-deficient, exhibited perinatal lethality, succumbing at approximately 2 wk to severe anemia (*SI Appendix*, Fig. S1). In contrast, $Nbn^{-/mid8vav}$ mice were viable and born at normal Mendelian ratios, indicating that the Nbn^{mid8} gene product is partially functional. $Nbn^{-/mid8}$ MEFs are inviable, and, before death, the cells exhibit severe genome instability and defective ATM activation (11). Hence, the viability of $Nbn^{-/mid8vav}$ BM components was unexpected, and suggested the possibility of underlying compensatory genetic changes.

Hematopoiesis was severely impaired in $Nbn^{-/mid8vav}$ mice and did not phenocopy $Atm^{-/-vav}$. Peripheral blood counts at 6 to 8 wk of age showed that both white blood cell (WBC) and red blood cell (RBC) numbers were decreased drastically in $Nbn^{-/mid8vav}$ compared with $Nbn^{-/+vav}$ mice: WBC, 8.66 ± 0.76 vs. 1.01 ± 0.14 ($\times 10^6$/mL); RBC, 9.99 ± 0.38 vs. 2.51 ± 0.62 ($\times 10^9$/mL) (Fig. 1 *A* and *B*). $Nbn^{-/mid8vav}$ mice exhibited a 2-fold elevation in platelet levels, likely a consequence of anemia (Fig. 1*C*). The percentage of both peripheral T cells and B cells also decreased in $Nbn^{-/mid8vav}$: T cell (percent), 36.4 and 26.7 vs. 0.4, 7.6, and 9.8; B cell (percent), 50.9 and 58.4 vs. 2.9, 1.6, and 8.3 (Fig. 1 *D* and *E*).

The cellularity of the thymus and BM was also markedly decreased in $Nbn^{-/mid8vav}$ mice (Fig. 1 *F* and *G*). Analysis of $Nbn^{-/mid8vav}$ BM was carried out at 6 to 8 wk of age. The percentages of B lineage cells ($B220^+$) and myeloid cell ($Mac\text{-}1^+$ and $Gr\text{-}1^+$) were decreased in $Nbn^{-/mid8vav}$ mice compared with $Nbn^{-/+vav}$. B and myeloid lineages were reduced by roughly 3-fold (B, 25.03% ± 1.47 vs. 7.23 ± 0.92; myeloid, 36.6% ± 2.83 vs. 14.32 ± 1.79). The levels of erythroid precursors ($Ter119^+$) were not changed (Fig. 2 *A*–*C*).

The depletion of B cell lineage cells appeared to coincide with onset of Ig gene assembly. Whereas pro-B cells ($CD43^+$) from $Nbn^{-/mid8vav}$ were increased (Fig. 2*E*), the levels of $B220^+$ cells

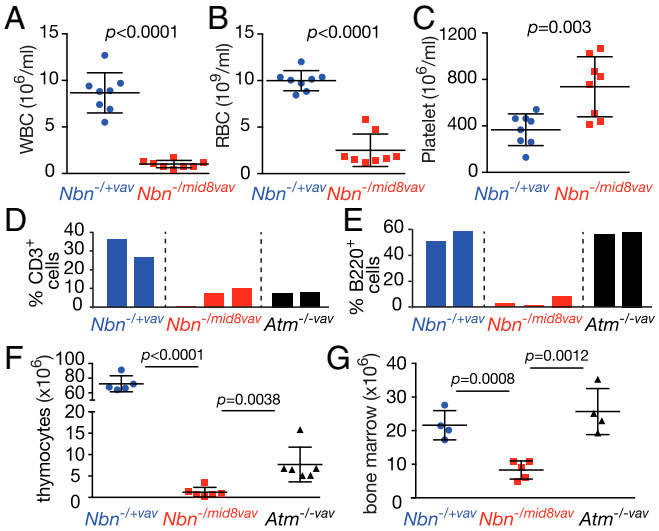

Fig. 1. $Nbn^{-/mid8vav}$ allele leads to hematopoiesis failure. (*A*–*C*) Peripheral blood counts analysis of $Nbn^{-/mid8vav}$ mice at 6 to 8 wk old. (*A*) WBC, (*B*) RBC, and (*C*) platelet; $n = 8$ mice of each genotype, mean ± SD, unpaired *t* test. (*D*) Percent $CD3^+$ cells from peripheral blood. (*E*) Percent $B220^+$ cells from peripheral blood. Each bar represents the data from an individual mouse. (*F*) The number of thymocytes decreases in $Nbn^{-/mid8vav}$ mice; $n = 5$ of $Nbn^{-/+vav}$, $n = 6$ of $Nbn^{-/mid8vav}$, $n = 6$ of $Atm^{-/-vav}$, 6 wk old, mean ± SD, unpaired *t* test. (*G*) The number of BM cells decreases in $Nbn^{-/mid8vav}$ mice; $n = 4$ of $Nbn^{-/+vav}$, $n = 5$ of $Nbn^{-/mid8vav}$, $n = 4$ of $Atm^{-/-vav}$, 6 wk-old, mean ± SD, unpaired *t* test.

decreased beginning at the pre-B stage when Ig heavy chain rearrangement commences (24, 25) to the immature B cell stage ($CD43^-$), and IgM^+ mature B cells were virtually undetectable (Fig. 2 *F*–*H*). These data suggest that $Nbn^{-/mid8vav}$ cells are unable to resolve DSBs formed during the course of B cell development, reminiscent of previous analyses of lymphocyte development in Mre11 complex mutants (19, 20, 26, 27). The hematopoietic phenotype of $Nbn^{-/mid8vav}$ mice is distinct from that of $Atm^{-/-vav}$ in all respects (Figs. 1 *E*–*G* and 2 *A*–*H*), underscoring the point that the $Nbn^{-/mid8vav}$ phenotype reflects the loss of both DSB repair functions and ATM activation.

$Nbn^{-/mid8vav}$ Mice Develop T Cell Lymphoma. In light of the predisposition to thymic lymphomas in $Atm^{-/-}$ mice, we monitored a cohort of $Nbn^{-/mid8vav}$ mice for 12 mo to assess the risk of malignancy. With 5.6 mo of mean tumor-free survival, 90% (18/20) of $Nbn^{-/mid8vav}$ mice developed hematologic malignancy, a significantly higher penetrance than that of $Atm^{-/-vav}$ mice (Fig. 3*A*). Most $Nbn^{-/mid8vav}$ tumors (17/18) were aggressive T cell lymphomas or leukemias (*SI Appendix*, Table S1) which became disseminated to the spleen (Fig. 3 *B*, *ii* and *iii*).

Whereas $Atm^{-/-vav}$ tumors exhibit a relatively immature phenotype ($CD3^{low}$ $CD4^+$ $CD8^+$) (28), $Nbn^{-/mid8vav}$ tumors were predominantly single positive ($CD8^+$) and the half of the cases examined were $CD3^{high}$ (*SI Appendix*, Fig. S2). Flow cytometric analysis of thymocyte at 6 wk of age reveal the $CD8^+$ population is elevated in $Nbn^{-/mid8vav}$ thymus compared with $Nbn^{-/+}$ or $Atm^{-/-}$ thymus before the emergence of malignant cells (*SI Appendix*, Fig. S3).

Genomic Analysis of Nbn^{mid8} T Cell Lymphoma. To gain insight regarding the underlying genetic changes that suppressed the lethality of the Nbn^{mid8} allele, we carried out genomic analyses of $Nbn^{-/mid8vav}$ tumors. Analysis of copy number variation (CNV) indicated the presence of multiple broad DNA copy number gains and losses, with recurrent CNV on chromosomes 9 and 15 (Fig. 4*A*). A focal amplification of 9qA2 was present in all tumors,

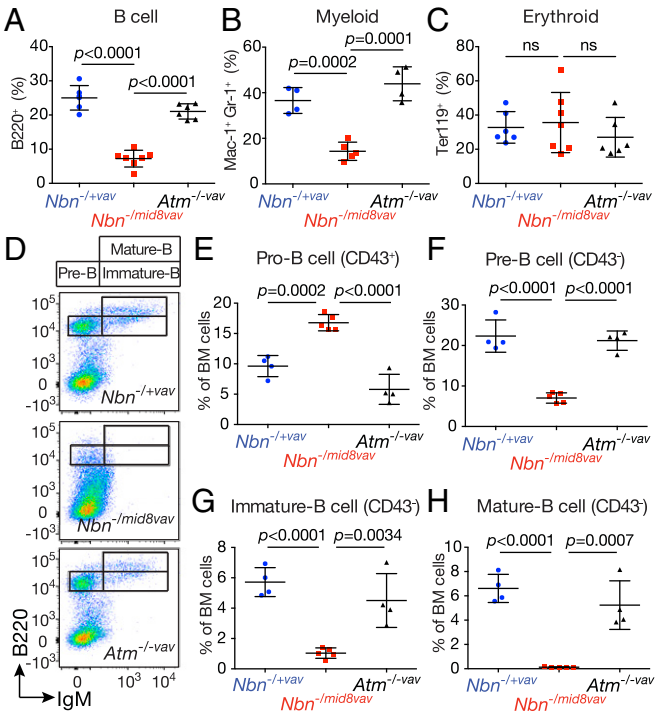

Fig. 2. Depletion of B cell lineage cells in $Nbn^{-/mid8vav}$ BM. (*A*) Percent B cell ($B220^+$ cells) from BM of indicated genotypes; $n = 5$ of $Nbn^{-/+vav}$, $n = 7$ of $Nbn^{-/mid8vav}$, $n = 6$ of $Atm^{-/-vav}$, mean ± SD, unpaired *t* test. (*B*) Percent myeloid cell (Mac-1^+ and Gr-1^+ cells) from BM of indicated genotypes; $n = 4$ of $Nbn^{-/+vav}$, $n = 5$ of $Nbn^{-/mid8vav}$, $n = 4$ of $Atm^{-/-vav}$, mean ± SD, unpaired *t* test. (*C*) Percent Erythroid cell ($Ter119^+$ cells) from BM of indicated genotypes; $n = 6$ of $Nbn^{-/+vav}$, $n = 7$ of $Nbn^{-/mid8vav}$, $n = 6$ of $Atm^{-/-vav}$, mean ± SD, unpaired *t* test, ns: not significant. (*D*) Representative scatter plot for B cell analysis of indicated genotypes. (*E*) Percent pro-B cells ($CD43^+$), (*F*) percent pre-B cells ($CD43^-$, $B220^+$, IgM^-), (*G*) percent immature B cells ($CD43^-$, $B220^+$, IgM^+), and (*H*) percent mature B cells ($CD43^-$, $B220^{+high}$, IgM^+) from BM of indicated genotypes; $n = 4$ of $Nbn^{-/+vav}$, $n = 5$ of $Nbn^{-/mid8vav}$, $n = 4$ of $Atm^{-/-vav}$, mean ± SD, unpaired *t* test.

albeit with variable amplitudes and breakpoints (*SI Appendix*, Fig. S4). This region includes the genes encoding *MRE11* and *CHK1*. Chromosome 9 amplification appears to be unique to $Nbn^{-/mid8vav}$ tumors, as amplification of this region has not been observed in thymic lymphomas from *TP53*- or *ATM*-deficient mice (28–30). Thus, the evolution of $Nbn^{-/mid8vav}$ malignancy is distinct.

Amplification was correlated with increased protein levels of Mre11 in $Nbn^{-/mid8}$ thymic tumors. Although there was no CNV for the *RAD50* gene, Rad50 protein levels were also increased (Fig. 4*B*). We propose that $Nbn^{-/mid8vav}$ cells select for amplification and overexpression of *MRE11* to compensate for the metastable interaction with the Nbn^{mid8} gene product and thereby permit cell survival. The increased levels of Mre11 in $Nbn^{-/mid8vav}$ tumors did not fully suppress the Nbn^{mid8} phenotype, as ionizing radiation (IR)-induced Kap1 S824 phosphorylation, an index of ATM activation, was not restored (Fig. 4*B*).

In this context, we sought to define when these 2 gene amplifications occurred in the transition to malignancy. We measured the copy numbers of genes that are present in chromosomes 9 or 15 at earlier times (4 and 9 wk old) before the age of tumor onset. Increased copy number of the *MRE11* and *CHK1* genes on chromosome 9 was detected in $Nbn^{-/mid8vav}$ thymocytes as early as 4 wk of age (1.46-fold for *MRE11*; 1.48-fold for *CHK1*), while the *NBN* copy number was not altered (Fig. 4*C*). *MYC* amplification on chromosome 15 was also detected in thymocytes of 4-wk-old $Nbn^{-/mid8vav}$ mice (1.38-fold), suggesting that amplifications on both chromosomes 9 and 15 occurred at an early stage in the leukemogenic process, presumably reflecting selection pressure for cell survival.

The finding of *CHK1* amplification in $Nbn^{-/mid8vav}$ T cell leukemias was reminiscent of the fact that human T cell acute lymphoblastic leukemia (T-ALL) exhibits *CHK1* overexpression, and is exquisitely sensitive to Chk1 inhibition (31). Because the *MRE11* and *CHK1* loci are linked on chromosome 9, it is unclear whether their respective copy number increases are independent events or occurred simultaneously.

Deep targeted sequencing of 578 key cancer-associated genes to identify potential drivers of T-ALL in $Nbn^{-/mid8vav}$ mice revealed that the mutational features of $Nbn^{-/mid8vav}$ tumors were consistent with those of T-ALL in humans and are similar, but not identical to, lymphomas arising in $Atm^{-/-}$ mice. The $Nbn^{-/mid8vav}$ leukemias uniformly contained activating mutations of *NOTCH1* which are mainly restricted to the proline, glutamic acid, serine, and threonine (PEST) domain of the Notch1 protein (*SI Appendix*, Table S2 and Fig. S5) as seen in human T-ALL (32). Amplification or activating mutations in *NOTCH1* have been also been noted in thymic lymphomas arising in *ATM*-deficient mice (28). Those lymphomas also contain trisomy 15, and $Nbn^{-/mid8vav}$ tumors similarly appear to have whole chromosome 15 duplications (Fig. 4*A*).

Beyond *NOTCH1*, mutations of other potential driver genes were found at various frequencies in $Nbn^{-/mid8vav}$ tumors (Fig. 4*D* and *SI Appendix*, Table S2). *TP53* mutations within the DNA binding domain were found with a high frequency, and were frequently biallelic due to loss of heterozygosity (Fig. 4*D* and *SI Appendix*, Fig. S5). The 2 mutations observed (S238P corresponding to human S241 and a truncation of oligomerization domain) affect DNA binding and p53-mediated cell growth suppression functions (33–36), suggesting that p53 deficiency may be a driver of $Nbn^{mid8vav}$ T-ALL. Other mutations also found in $Nbn^{-/mid8vav}$ tumors include *ARID5b*, *BCL6*, *BCOR*, and *IKZF1* (Fig. 4*D* and *SI Appendix*, Table S2).

Rescue of Nbn^{mid8} MEFs Lethality. To test the interpretation that *MRE11* amplification and overexpression are compensatory changes that can suppress Nbn^{mid8} lethality, we overexpressed the murine *MRE11* cDNA in $Nbn^{flox/mid8}$ *creERT2* MEFs (11). In these cells, *cre* expression is activated by tamoxifen (4-OHT) to effect inactivation of the (wild-type) Nbn^{flox} allele to create $Nbn^{-/mid8}$ cells. *MRE11*-expressing $Nbn^{flox/mid8}$ *creERT2* MEFs were treated with 4-OHT for 48 h, and plated. However, we

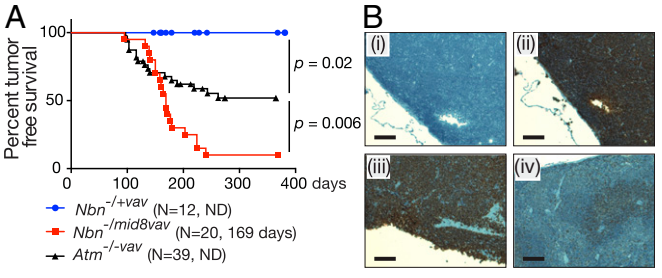

Fig. 3. $Nbn^{-/mid8vav}$ mice develops spontaneous T cell lymphoma. (*A*) Mouse tumor-free survival. Each data point represents the percent survival of mice with $Nbn^{-/+vav}$ and $Nbn^{-/mid8vav}$ at a given age. N denotes total number of mice for each genotype, and the average age in death in days is shown. ND means not determined. Note that the $Atm^{-/-vav}$ survival curve was previously established in our colony and reported. Data from ref. 19. (*B*) CD3 immunohistochemistry of thymus (*i* and *ii*) and spleen (*iii* and *iv*); control IgG (*i*), CD3 antibody (*ii*, *iii*, and *iv*), thymus (*i* and *ii*), and spleen (*iii*) from tumor-bearing $Nbn^{-/mid8vav}$ mouse; and spleen (*iv*) from littermate $Nbn^{-/+vav}$ mouse. (Scale bars, 100 μm.)

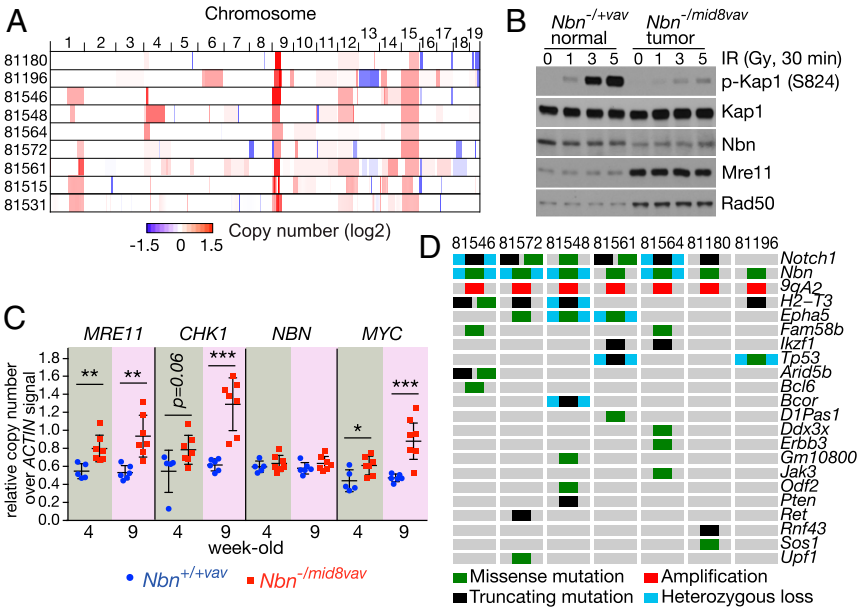

Fig. 4. Genomic analysis of $Nbn^{-/mid8vav}$ T cell lymphoma. (*A*) Heatmap of CNV of 9 thymic tumors lymphomas from $Nbn^{-/mid8vav}$ mice. Analysis was performed using whole genome sequencing or deep targeted sequencing of 578 key cancer-associated genes. (*B*) Western blot for ATM signaling and the levels of Mre11 complex in $Nbn^{-/mid8vav}$ thymic tumors. IR-induced phosphorylation of Kap1 (S824) was assessed upon different doses of IR as indicated. (*C*) CNV of *MRE11*, *CHK1*, *NBN*, and *MYC* genes from thymocytes of wild-type and $Nbn^{-/mid8vav}$ mice at the ages of 4 and 9 wk. Relative copy numbers for genes over *ACTIN* signals of each biological sample are shown; $n = 5$ of $Nbn^{+/+vav}$ (4 wk old), $n = 7$ of $Nbn^{-/mid8vav}$ (4 wk old), $n = 6$ of $Nbn^{+/+vav}$ (9 wk old), $n = 7$ of $Nbn^{-/mid8vav}$ (9 wk old), mean ± SD, unpaired *t* test (*$P < 0.05$; **$P < 0.01$; ***$P < 0.001$). (*D*) Oncoprint of genomic alterations of $Nbn^{-/mid8vav}$ T cell lymphoma. Note that *Nbn* mutation is Nbn^{mid8} allele (N682_K685del). Complete mutation list is presented in *SI Appendix*, Table S1. The mouse identification numbers are indicated (in *A* and *D*).

were unable to establish viable colonies of *MRE11*-expressing $Nbn^{-/mid8}$ cells.

As noted above, the Mre11 complex plays an integral role in DNA replication (1, 9). On that basis, we tested the hypothesis that the coamplification of the *CHK1* locus uniformly observed (Fig. 4 *A* and *C*) is an obligate event for viability of $Nbn^{-/mid8vav}$ cells. Therefore, *CHK1* and *MRE11* were cooverexpressed to determine whether this would rescue $Nbn^{-/mid8}$ lethality. After deletion of the conditional *NBN* allele, cell clones which were $Nbn^{-/mid8}$ but overexpressed *CHK1* and *MRE11* emerged (hereafter referred to as $Nbn^{-/mid8}$ CM). Three independent $Nbn^{-/mid8}$ CM clones (2, 7, and 8) were verified by PCR genotyping, and RT-PCR/sequencing confirmed that the sole source of RNA for Nbn protein is Nbn^{mid8} mutant allele (*SI Appendix*, Fig. S6).

The $Nbn^{-/mid8}$ CM clones exhibited slower growth than the parental $Nbn^{flox/mid8}$ CM cells (Fig. 5*A*). Mre11 and Chk1 levels were increased in 3 $Nbn^{-/mid8}$ CM clones (Fig. 5*B*). We also found that, in clone 2, Nbn levels were increased (Fig. 5*B*) due to 7.7-fold amplification of the Nbn^{mid8} locus (Fig. 5*C*), likely in response to selective pressure imposed by the impaired interaction of Mre11 and Nbn^{mid8}.

To assess whether *MRE11* and *CHK1* overexpression alleviates DNA damage occurring in $Nbn^{-/mid8}$ cells, we compared γH2AX foci and metaphase spreads in cells overexpressing either *MRE11* or *CHK1* alone or in combination. Five days after deletion of the conditional *NBN* allele, the ensuing $Nbn^{-/mid8}$ cells exhibited multiple indices of DNA damage such as γH2AX foci and chromosomal aberrations (Fig. 5 *D* and *E*). Overexpression of *MRE11* and *CHK1* in combination mitigated those outcomes, reducing γH2AX, 41.8% vs. 19.7%, and metaphase aberrations, 43.8% vs. 20% (Fig. 5 *D* and *E*). Whereas *CHK1* overexpression alone had no effect, *MRE11* overexpression alone was sufficient to reduce DNA damage in $Nbn^{-/mid8}$ cells (Fig. 5 *D* and *E*) even though *MRE11*-expressing $Nbn^{-/mid8}$ cells were not ultimately viable. This indicates that, although overexpression of *MRE11* was sufficient to alleviate some of genomic instability by Nbn^{mid8} allele, coincident *CHK1* overexpression was required for cell viability.

Discussion

In the previous work, we established evidence that the essential function of Nbn was to stabilize and promote proper assembly and function of the Mre11 complex using biochemical approaches and atomic force microscopy. In $Nbn^{-/mid8}$ cells, Mre11 complex components are present at essentially normal levels, but Nbn^{mid8} interaction with Mre11 is compromised, abolishing ATM activation and blocking viability (11). In this study, we used the context of hematopoietic development to assess whether Nbn^{mid8} retained residual function.

Whereas Nbn deficiency in the BM led to perinatal lethality due to anemia, $Nbn^{-/mid8vav}$ mice were viable, with a median lifespan of 169 d. $Nbn^{-/mid8vav}$ succumbed to a highly aggressive T cell malignancy that bore some hallmarks of T-ALL in humans. Genomic analysis of $Nbn^{-/mid8vav}$ cancers revealed copy number gains and overexpression of *MRE11* and *CHK1* in 100% of tumors analyzed. We were able to establish clonal $Nbn^{-/mid8}$ MEF cell lines only upon cooverexpression of *MRE11* and *CHK1*, demonstrating that increased levels of both was required to suppress Nbn^{mid8} lethality.

Mre11 Complex Assembly and Tumor Suppression. Each member of the Mre11 complex is essential, and none appear to function outside of the complex. Nevertheless, Nbn plays a distinct role in Mre11 complex stability. For example, mutations that reduce Nbn levels do not grossly alter the levels of Mre11 and Rad50 (13, 14), whereas the stabilities of Mre11 and Rad50 are interdependent, so that mutations destabilizing either reduce the level of the other (4, 37). Hence, Mre11 and Rad50, which are present in all clades of life, constitute the core of the Mre11 complex, while Nbn, seen only in Eukarya, has evolved to promote proper assembly and activity of the complex.

We propose that this function of Nbn underlies the selection for *MRE11* amplification and overexpression in $Nbn^{-/mid8vav}$ tumors. Based on principles of ligand binding equilibria, the weakened interaction between Nbn^{mid8} and Mre11 would be partially mitigated if the levels of either Mre11 or Nbn^{mid8} were elevated. This could increase the steady-state level of productively assembled complexes to a threshold that would permit viability. Supporting this concept, in $Nbn^{-/mid8}$ CM clone 2, the Nbn^{mid8} locus was also amplified and overexpressed (Fig. 5 *B* and *C*). This suppression is not complete, as the defect in IR-induced Kap1 S824 phosphorylation of $Nbn^{-/mid8vav}$ tumors was not rescued (Fig. 4*B*). We interpret this to mean that the levels of putatively assembled complexes were insufficient to allow for IR-induced ATM activation.

Several mouse models of Mre11 complex hypomorphism have been described (9). No predisposition to malignancy has been

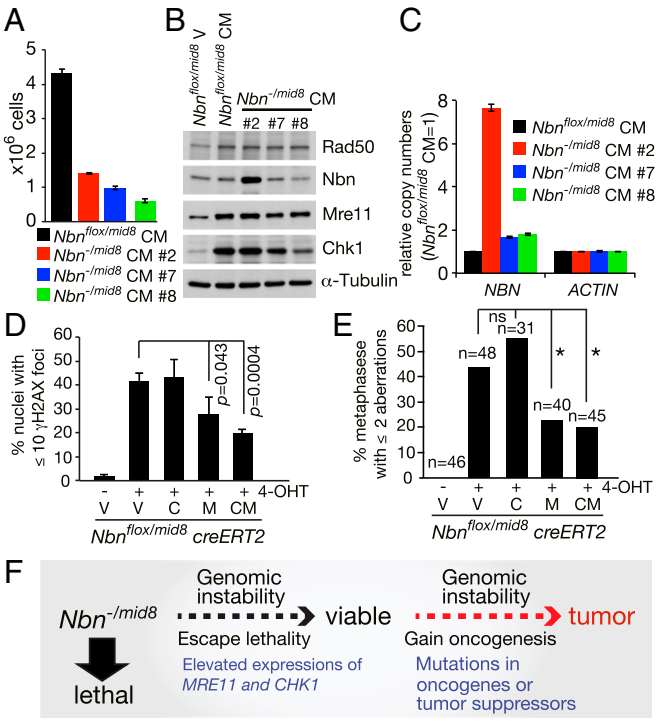

Fig. 5. Increased expression of *MRE11* and *CHK1* genes rescues $Nbn^{-/mid8}$ MEFs from lethality. (*A*) Growth of 3 different stable clones of $Nbn^{-/mid8}$ MEFs expressing both exogenous *MRE11* and *CHK1*. $Nbn^{flox/mid8}$ CM is a parental cell. Cells were plated (2×10^4) and counted at day 4, mean ± SD, triplicates. Hereafter, V, C, and M denote empty *VECTOR*, *CHK1*, and *MRE11*, respectively. (*B*) Western blots show the levels of Mre11, Rad50, Nbn, and Chk1 in 3 stable $Nbn^{-/mid8}$ CM clones. $Nbn^{flox/mid8}$ CM is parental cells. (*C*) *NBN* gene amplification occurs in clone 2 of $Nbn^{-/mid8}$ CM. (*D* and *E*) Genomic instability in $Nbn^{-/mid8}$ MEFs was alleviated by ectopic expression of *MRE11*. (*D*) Percentage nuclei with ≤ 10 γH2AX foci and (*E*) metaphases with ≤ 2 aberrations were measured in $Nbn^{flox/mid8}$ *CreERT2* MEFs expressing either *MRE11* and *CHK1* alone or in combination, 5 d post–4-OHT treatments. *P* value was determined by unpaired *t* test, mean ± SD, total more than 800 nuclei counted from 3 independent experiments for γH2AX foci (in *D*) and Fisher's exact test, $*P < 0.05$, ns: not significant (in *E*). (*F*) Summary of T cell lymphomagenesis in $Nbn^{-/mid8vav}$ mice. Gross genomic instability of $Nbn^{-/mid8}$ T cells causes impairment in cell proliferation and developmental defects. Few cells that spontaneously gain *MRE11* and *CHK1* amplification escape from the cellular lethality. By acquiring additional tumor-prone mutations, these cells can transform into thymic lymphoma.

observed in these mutants, although, in some cases, the latency of tumorigenesis associated with *TP53* or *CHK2* mutations is reduced; presumably, this reflects the combined effect of genome instability and checkpoint defects associated with those mutations. However, the strong cancer predisposition seen in $Nbn^{-/mid8vav}$ is distinct from other Mre11 complex single mutants, and phenocopies that of $Nbn^{\Delta B/\Delta B}$ $Atm^{-/-\ vav}$ mice. Two features of these mice likely underlie the similar outcomes (19). First, ATM activity is virtually absent in the former and completely absent in the latter, which means that, in both contexts, DNA damage-dependent cell cycle checkpoints and apoptotic induction are compromised. Second, both exhibit high degrees of genomic instability, which likely increases the probability of chromosome rearrangement and/or mutations that enhance progression to the malignant phenotype.

The Requirement for *CHK1* Overexpression. In $Nbn^{-/mid8}$ MEFs, overexpression of *MRE11* alone is not sufficient to restore viability. Cooverexpression of *CHK1* is required to obtain stable clones (Fig. 5*B*). This finding strongly suggests that amplification and overexpression of the *MRE11* and *CHK1* loci in $Nbn^{-/mid8vav}$ T-ALL cells reflects the same requirement. Significantly increased copy numbers of both loci were observed as early as 4 wk of age, supporting the interpretation that the overexpression of both genes is required for viability, irrespective of the malignant phenotype.

Whereas *MRE11* overexpression in $Nbn^{-/mid8}$ MEFs mitigated the gross chromosome instability observed after *cre*-mediated deletion of the Nbn^{flox} allele (Fig. 5*E*), the requirement for *CHK1* overexpression suggests an additional stress is imposed by the Nbn^{mid8}-containing Mre11 complex. It is likely that with the ATM–Mre11 complex axis of the DDR crippled by the Nbn^{mid8} allele, selection for *CHK1* overexpression is imposed by the genomic instability associated with severe Mre11 complex hypomorphism. In this scenario, Chk1 function may mitigate the lethal effects of DNA damage in parallel with its normal role in the response to DNA replication stress.

DNA replication stress, broadly defined as a state in which progression of the replisome is impaired by DNA lesions or insufficiency of the nucleotide pool, is an important source of DNA damage in proliferating cells. DNA replication stress also appears to be intrinsic to the premalignant and malignant phenotypes (38, 39). The viability of cells experiencing DNA replication stress is largely dependent on the ATR–Chk1 axis of the DDR (40, 41), and so the development of Chk1 and ATR inhibitors has emerged as a priority in cancer therapeutics (42).

Given its requirement for preserving genomic integrity during S phase (6), it is also conceivable that the selection for *CHK1* overexpression reflects that Mre11 complex depletion causes DNA replication stress in a manner analogous to depletion of MCM proteins and other replisome components (43), a state that acutely requires Chk1 activity to maintain viability (39, 40).

Cytologic analyses of acute Nbn depletion in MEFs offered the suggestion that the Mre11 complex's role in resolving DNA replication intermediates underlies its essentiality (44). Consistent with that view, we have shown that Mre11 complex foci arise during unperturbed S phase. Those foci do not colocalize with DSB markers such as γH2AX or BRCA1, but colocalize with PCNA throughout S phase (7, 8). Hence, they do not appear to be associated with DSBs and could potentially represent DNA replication intermediates that precede fork collapse and DSB formation.

An additional possibility is that the Mre11 complex is situated at the fork to degrade secondary structures on the lagging strand and thereby drive sister chromatid recombination, as has been suggested in bacteria and *S. cerevisiae* (45–47). Whatever the source of the initiating DSBs, the Mre11 complex is acutely required for sister chromatid recombination (9), a function that could also account for Chk1 activation upon depletion as well as the complex's association with the fork under normal conditions.

***Nbn*$^{-/mid8vav}$ and T-ALL in Humans.** Genomic analysis of Nbn^{mid8} leukemias revealed a similar pattern of mutations to that found in human T-ALL (31, 32). The *NOTCH1* mutations were found in 6 tumors out of 7 samples analyzed, and the mutations were restricted to the PEST domain, as seen in human T-ALL and also T-ALL arising in $Atm^{-/-vav}$ mice (28, 32). This suggests that *NOTCH1* mutations could be the main driver for T-ALL tumors. Other known human tumor mutations were also found in the $Nbn^{-/mid8vav}$ leukemias. For example, *BCL6*, *BCOR*, and *IKZF1* are the genes found mutated in human T-ALL and B-ALL (48–53). *BCL6* is a regulator for germinal center reaction and found deregulated in ∼40% diffuse large B cell lymphomas by translocation (48, 52). Loss of function mutations in *BCOR* has been noted in hematopoietic malignancies (49, 50). In this regard, $Nbn^{-/mid8vav}$ may provide an in vivo model for examining the contributions of the various driver mutations in T-ALL and other malignancies in the context of Mre11 complex hypomorphism.

The Mre11 complex plays a critical role in preventing oncogene-induced carcinogenesis in mammary epithelium (54). It is conceivable that Mre11 complex hypomorphism in $Nbn^{-/mid8vav}$ cells similarly creates a permissive state for oncogene-driven proliferation and malignancy. The data presented here reveal that Nbn meets the definition of a tumor suppressor in hematopoietic cells via its role in ATM activation and in DNA repair. Therefore, the tumor-suppressive functions defined in the epithelium appear to be recapitulated in the hematopoietic compartment. Further examination of genetic interactions between Mre11 complex hypomorphism and oncogenic driver mutations in hematologic malignancy will shed light on the mechanisms underlying the tumor-suppressive role of the Mre11 complex in this context.

Materials and Methods

All mouse works were carried out according to the protocol approved by the Institutional Animal Care and Use Committee of Memorial Sloan-Kettering (MSK) Cancer Center. For more information on mice, sequencing and analysis, histology, cell lines, peripheral blood analysis, flow cytometry, cellular assays, copy number qPCR, and reagents, please consult *SI Appendix, Supplementary Materials and Methods*.

ACKNOWLEDGMENTS. We thank Fred Alt for Atm^{flox} mice, Matthias Stadtfeld and Thomas Graf for vav^{cre} mice, the MSK Integrated Genomics Operation, and members of the J.H.J.P. lab, including Thomas J. Kelly for helpful discussion throughout the course of this study. This work was supported by GM59413 (J.H.J.P), U54 OD020355 (J.H.J.P and B.S.T.), R01 CA207244 (B.S.T.), and R01 CA204749 (B.S.T.), and the American Cancer Society (RSG-15-067-01-TBG), Anna Fuller Fund, the Josie Robertson Foundation (B.S.T.), the Cycle for Survival, and the MSK Cancer Center Core Grant P30 CA008748.

1. A. Syed, J. A. Tainer, The MRE11-RAD50-NBS1 complex conducts the orchestration of damage signaling and outcomes to stress in DNA replication and repair. *Annu. Rev. Biochem.* **87**, 263–294 (2018).
2. R. Varon *et al*., Nibrin, a novel DNA double-strand break repair protein, is mutated in Nijmegen breakage syndrome. *Cell* **93**, 467–476 (1998).
3. R. Waltes *et al*., Human RAD50 deficiency in a Nijmegen breakage syndrome-like disorder. *Am. J. Hum. Genet.* **84**, 605–616 (2009).
4. G. S. Stewart *et al*., The DNA double-strand break repair gene hMRE11 is mutated in individuals with an ataxia-telangiectasia-like disorder. *Cell* **99**, 577–587 (1999).
5. B. M. Sirbu *et al*., Identification of proteins at active, stalled, and collapsed replication forks using isolation of proteins on nascent DNA (iPOND) coupled with mass spectrometry. *J. Biol. Chem.* **288**, 31458–31467 (2013).
6. C. A. Adelman, S. De, J. H. Petrini, Rad50 is dispensable for the maintenance and viability of postmitotic tissues. *Mol. Cell. Biol.* **29**, 483–492 (2009).
7. O. K. Mirzoeva, J. H. Petrini, DNA replication-dependent nuclear dynamics of the Mre11 complex. *Mol. Cancer Res.* **1**, 207–218 (2003).
8. R. S. Maser *et al*., Mre11 complex and DNA replication: Linkage to E2F and sites of DNA synthesis. *Mol. Cell. Biol.* **21**, 6006–6016 (2001).
9. T. H. Stracker, J. H. Petrini, The MRE11 complex: Starting from the ends. *Nat. Rev. Mol. Cell Biol.* **12**, 90–103 (2011).
10. C. B. Schiller *et al*., Structure of Mre11-Nbs1 complex yields insights into ataxia-telangiectasia-like disease mutations and DNA damage signaling. *Nat. Struct. Mol. Biol.* **19**, 693–700 (2012).
11. J. H. Kim *et al*., The Mre11-Nbs1 interface is essential for viability and tumor suppression. *Cell Rep.* **18**, 496–507 (2017).
12. Y. Shiloh, Ataxia-telangiectasia and the Nijmegen breakage syndrome: Related disorders but genes apart. *Annu. Rev. Genet.* **31**, 635–662 (1997).
13. J. P. Carney *et al*., The hMre11/hRad50 protein complex and Nijmegen breakage syndrome: Linkage of double-strand break repair to the cellular DNA damage response. *Cell* **93**, 477–486 (1998).
14. B. R. Williams *et al*., A murine model of Nijmegen breakage syndrome. *Curr. Biol.* **12**, 648–653 (2002).
15. J. Kobayashi *et al*., NBS1 localizes to gamma-H2AX foci through interaction with the FHA/BRCT domain. *Curr. Biol.* **12**, 1846–1851 (2002).
16. J. Lloyd *et al*., A supramodular FHA/BRCT-repeat architecture mediates Nbs1 adaptor function in response to DNA damage. *Cell* **139**, 100–111 (2009).
17. R. S. Williams *et al*., Nbs1 flexibly tethers Ctp1 and Mre11-Rad50 to coordinate DNA double-strand break processing and repair. *Cell* **139**, 87–99 (2009).
18. J. R. Chapman, S. P. Jackson, Phospho-dependent interactions between NBS1 and MDC1 mediate chromatin retention of the MRN complex at sites of DNA damage. *EMBO Rep.* **9**, 795–801 (2008).
19. A. Balestrini *et al*., Defining ATM-independent functions of the Mre11 complex with a novel mouse model. *Mol. Cancer Res.* **14**, 185–195 (2016).
20. E. Callén *et al*., ATM prevents the persistence and propagation of chromosome breaks in lymphocytes. *Cell* **130**, 63–75 (2007).
21. B. Reina-San-Martin, M. C. Nussenzweig, A. Nussenzweig, S. Difilippantonio, Genomic instability, endoreduplication, and diminished Ig class-switch recombination in B cells lacking Nbs1. *Proc. Natl. Acad. Sci. U.S.A.* **102**, 1590–1595 (2005).
22. I. Demuth *et al*., An inducible null mutant murine model of Nijmegen breakage syndrome proves the essential function of NBS1 in chromosomal stability and cell viability. *Hum. Mol. Genet.* **13**, 2385–2397 (2004).
23. M. Stadtfeld, T. Graf, Assessing the role of hematopoietic plasticity for endothelial and hepatocyte development by non-invasive lineage tracing. *Development* **132**, 203–213 (2005).
24. F. W. Alt, Y. Zhang, F. L. Meng, C. Guo, B. Schwer, Mechanisms of programmed DNA lesions and genomic instability in the immune system. *Cell* **152**, 417–429 (2013).
25. G. Teng, D. G. Schatz, Regulation and evolution of the RAG recombinase. *Adv. Immunol.* **128**, 1–39 (2015).
26. L. Deriano, T. H. Stracker, A. Baker, J. H. Petrini, D. B. Roth, Roles for NBS1 in alternative nonhomologous end-joining of V(D)J recombination intermediates. *Mol. Cell* **34**, 13–25 (2009).
27. B. A. Helmink *et al*., MRN complex function in the repair of chromosomal Rag-mediated DNA double-strand breaks. *J. Exp. Med.* **206**, 669–679 (2009).
28. S. Zha *et al*., ATM-deficient thymic lymphoma is associated with aberrant tcrd rearrangement and gene amplification. *J. Exp. Med.* **207**, 1369–1380 (2010).
29. C. Dudgeon *et al*., The evolution of thymic lymphomas in p53 knockout mice. *Genes Dev.* **28**, 2613–2620 (2014).
30. P. C. Genik *et al*., Strain background determines lymphoma incidence in Atm knockout mice. *Neoplasia* **16**, 129–136 (2014).
31. L. M. Sarmento *et al*., CHK1 overexpression in T-cell acute lymphoblastic leukemia is essential for proliferation and survival by preventing excessive replication stress. *Oncogene* **34**, 2978–2990 (2015).
32. A. P. Weng *et al*., Activating mutations of NOTCH1 in human T cell acute lymphoblastic leukemia. *Science* **306**, 269–271 (2004).
33. C. G. Maki, Oligomerization is required for p53 to be efficiently ubiquitinated by MDM2. *J. Biol. Chem.* **274**, 16531–16535 (1999).
34. P. Monti *et al*., Tumour p53 mutations exhibit promoter selective dominance over wild type p53. *Oncogene* **21**, 1641–1648 (2002).
35. S. Rajagopalan, A. Andreeva, T. J. Rutherford, A. R. Fersht, Mapping the physical and functional interactions between the tumor suppressors p53 and BRCA2. *Proc. Natl. Acad. Sci. U.S.A.* **107**, 8587–8592 (2010).
36. N. W. Fischer, A. Prodeus, D. Malkin, J. Gariépy, p53 oligomerization status modulates cell fate decisions between growth, arrest and apoptosis. *Cell Cycle* **15**, 3210–3219 (2016).
37. J. W. Theunissen *et al*., Checkpoint failure and chromosomal instability without lymphomagenesis in Mre11(ATLD1/ATLD1) mice. *Mol. Cell* **12**, 1511–1523 (2003).
38. M. Macheret, T. D. Halazonetis, DNA replication stress as a hallmark of cancer. *Annu. Rev. Pathol.* **10**, 425–448 (2015).
39. H. Gaillard, T. García-Muse, A. Aguilera, Replication stress and cancer. *Nat. Rev. Cancer* **15**, 276–289 (2015).
40. D. W. Schoppy *et al*., Oncogenic stress sensitizes murine cancers to hypomorphic suppression of ATR. *J. Clin. Invest.* **122**, 241–252 (2012).
41. M. K. Zeman, K. A. Cimprich, Causes and consequences of replication stress. *Nat. Cell Biol.* **16**, 2–9 (2014).
42. P. G. Pilie, C. Tang, G. B. Mills, T. A. Yap, State-of-the-art strategies for targeting the DNA damage response in cancer. *Nat. Rev. Clin. Oncol.* **16**, 81–104 (2019).
43. S. A. Hills, J. F. Diffley, DNA replication and oncogene-induced replicative stress. *Curr. Biol.* **24**, R435–R444 (2014). Erratum in: *Curr. Biol.* **24**, 1563 (2014).
44. C. Bruhn, Z. W. Zhou, H. Ai, Z. Q. Wang, The essential function of the MRN complex in the resolution of endogenous replication intermediates. *Cell Rep.* **6**, 182–195 (2014).
45. J. C. Connelly, D. R. Leach, The sbcC and sbcD genes of *Escherichia coli* encode a nuclease involved in palindrome inviability and genetic recombination. *Genes Cells* **1**, 285–291 (1996).
46. J. C. Connelly, L. A. Kirkham, D. R. Leach, The SbcCD nuclease of *Escherichia coli* is a structural maintenance of chromosomes (SMC) family protein that cleaves hairpin DNA. *Proc. Natl. Acad. Sci. U.S.A.* **95**, 7969–7974 (1998).
47. K. S. Lobachev, D. A. Gordenin, M. A. Resnick, The Mre11 complex is required for repair of hairpin-capped double-strand breaks and prevention of chromosome rearrangements. *Cell* **108**, 183–193 (2002).
48. M. P. Butler *et al*., Alternative translocation breakpoint cluster region 5′ to BCL-6 in B-cell non-Hodgkin's lymphoma. *Cancer Res.* **62**, 4089–4094 (2002).
49. F. Damm *et al*., BCOR and BCORL1 mutations in myelodysplastic syndromes and related disorders. *Blood* **122**, 3169–3177 (2013).
50. V. Grossmann *et al*., Whole-exome sequencing identifies somatic mutations of BCOR in acute myeloid leukemia with normal karyotype. *Blood* **118**, 6153–6163 (2011).
51. P. Kastner, S. Chan, Role of Ikaros in T-cell acute lymphoblastic leukemia. *World J. Biol. Chem.* **2**, 108–114 (2011).
52. F. Lo Coco *et al*., Rearrangements of the BCL6 gene in diffuse large cell non-Hodgkin's lymphoma. *Blood* **83**, 1757–1759 (1994).
53. C. G. Mullighan *et al*., BCR-ABL1 lymphoblastic leukaemia is characterized by the deletion of Ikaros. *Nature* **453**, 110–114 (2008).
54. G. P. Gupta *et al*., The Mre11 complex suppresses oncogene-driven breast tumorigenesis and metastasis. *Mol. Cell* **52**, 353–365 (2013).